Astronomy & Astrophysics manuscript no. main
May 15, 2024

The variability of Betelgeuse explained by surface convection

Q. Pilate[1], A. López Ariste[1], A. Lavail[1], Ph. Mathias[1]

IRAP, Université de Toulouse, CNRS, CNES, UPS. 14, Av. E. Belin. 31400 Toulouse, France

Received ...; accepted ...

ABSTRACT

Key words.

1. Introduction

Betelgeuse is a prototypical red supergiant (RSG), known to be a semi-regular variable. Several periods can be found in the literature, usually clustered around the so-called long secondary period (LSP) of 2000 d, plus shorter periods around 400 and 200 d (Kiss et al. 2006). The origin of the LSP remains a source of discussion: some have tried to find the explanation of the LSP in the lifetime of the large convective cells present at the surface of RSG (e.g Stothers 2010) while others have invoked a magnetic field (Wood et al. 2004). The shorter periods of 400 and 200 d seem to have a different origin than the LSP. By studying a large sample of RSGs, Kiss et al. (2006) attributed the 400 d period to radial pulsation modes, while the 200 d period being attributed to the first overtone (Joyce et al. 2020), in agreement with the historical work of Stothers (1969).

Besides radial pulsation, surface activity leading to random brightness variation has also been mentioned to explain the variability of Betelgeuse, firstly theorised by Schwarzschild (1975). More recently, Gray (2008) proposed that the 400 d period was a consequence of convective activity. Betelgeuse is known to present large convective cells with lifetimes of the order of one to two years (López Ariste et al. 2018) and measurable changes within the span of one week. Bright convection cells near the disk center will increase the integrated brightness of the star compared with other situations where such cells are found near the edges. So, even without invoking the formation of dust or other changes in opacity, one may argue that the simple evolution of convective patterns of the star may create variability. Such variability could be expected to be random, but will present quasi-periodicities related to the typical time scales of the convective patterns (Gray 2008).

At the end of 2019, Betelgeuse reached a historical minimum in its luminosity, called the Great Dimming (Guinan et al. 2020). From interferometric and spectroscopic data, it has been proposed that this event was caused by the formation of a cloud of dust close to the line of sight (Montargès et al. 2021). Interferometric images show a drop in luminosity in the southern hemisphere of Betelgeuse, which could be caused by a mass loss event and leading to this dimming (Dupree et al. 2022). Other hypotheses have also been explored, such as a drop in temperature (Harper et al. 2020), or an increase in the molecular opacity (Kravchenko et al. 2021). In this event, it turns out that a change in brightness may not be due to pulsation but to a change in the brightness distribution over the stellar disk. Since the end of the Great Dimming event, Betelgeuse has continue its random variation of brightness. But quite interestingly, it has been shown by Jadlovský et al. (2023) and Dupree et al. (2022) that the periodicity of Betelgeuse has changed since the dimming. Using the light curves from AAVSO, the cited authors showed that before the dimming, the dominant period of Betelgeuse was the 400 d period, while after the great dimming, the main periods of Betelgeuse have shortened, oscillating between 97 d and 230 d (Dupree et al. 2022), revealing a change in the behaviour of the atmosphere of Betelgeuse. While the great dimming may be seen as a singular event, such modifications of the variability periods bring up the question of whether all changes in brightness can be due to similar changes in the brightness distribution over the disk and unrelated to any pulsation phenomenon. Our interest in an alternative explanation of the variability in terms of convective patterns arose. In order to address this question, we seek such typical periods of 400 and 200 d in observational proxies related to the convective activity but not to any pulsation, such as the linear polarization spectra.

Linear polarization in the atomic lines of the spectrum of Betelgeuse, discovered by Aurière et al. (2016), has been interpreted as the joint action of two mechanisms. First, the depolarization of the continuum by atoms which absorb linearly polarized light from the continuum and re-emit unpolarized light, the continuum photons being polarized by Rayleigh scattering. This depolarization produces signals with circular symmetry over the visible disk, which would cancel out the net linear polarization on a homogeneous disk. Thus, such mechanism of polarization must be combined with an inhomogeneous disk to produce the net linear polarization signal observed. This interpretation suggested the possibility of mapping those brightness inhomogeneities. This has been achieved by López Ariste et al. (2018), who produced even 3-dimensional images of the atmosphere of Betelgeuse (López Ariste et al. 2022) by taking advantage of the different heights of formation of different lines in the spectrum of Betelgeuse. The produced images compare very well with contemporaneous images made with interferometric techniques (Montargès et al. 2016) and show clear convective patterns, akin to solar granulation.

Linear polarization observed in the atomic lines is therefore a proxy of convection, a priori unrelated to radial pulsations but linked to the brightness inhomogeneities due to the convective patterns in Betelgeuse. If one can find the aforementioned variability periods in linear polarization, we must conclude that these periods are related to the convective activity which originates the linear polarization signals. This is the purpose of the present work.

In section 2, we describe the dataset of linear polarization obtained with Narval and Neo-Narval at TBL, as well as the Lomb-Scargle periodograms used to derive periods. In section 3, we seek periods in the LSD profiles of Betelgeuse using the Lomb-Scarlge periodogram. In section 4, we associate the 200 d period with the convective timescale of the smallest granules and the 330 d periodicity with the largest granules. We speculate on an explanation in the change of variability of Betelgeuse before and after the great dimming.

2. The polarimetric data

Betelgeuse has been observed for the last 10 years with Narval and Neo-Narval at the Telescope Bernard Lyot[1]. These two instruments measure the polarization over the visible and near infrared spectra of Betelgeuese (390-1000 nm) with high spectral resolution (R=65000) and high polarimetric sensitivity. The signal-to-noise ratios are not sufficient to measure the weak polarization signals in individual atomic lines of the spectrum. These amplitudes are known to be of the order of 10^{-4} times the continuum intensity, and they only exceptionally reach amplitudes of 10^{-3}. In those observations, enough photons can be accumulated per spectral bin to detect the linear polarization signal above noise in lines (Aurière et al. 2016). Most commonly, the amplitudes of linear polarization are below noise levels. On those occasions, we have to add up the signals of thousands of lines to increase the signal-to-noise ratios. This addition is performed through a technique called Least-Squares Deconvolution (LSD) (Donati et al. 1997).This technique has been successfully used in the past to measure magnetic field distributions over stellar surfaces and is now employed to produce images of the brightness distributions in the photosphere of Betelgeuse and other RSGs, as cited in the Introduction.

In this work, we shall examine the signals produced through the LSD technique, which produce a pseudo-spectral line in intensity and linear polarization. This pseudo-spectral line does not correspond to any particular atomic species but rather represents an average of all species present and emitting in the photosphere of Betelgeuse. Following these procedures of line addition, the resulting profiles carry the coherent signals present in the photospheric lines, but the specific characteristics of individual spectral lines are erased. All of this data has been previously presented before by Aurière et al. (2016), Mathias et al. (2018) and López Ariste et al. (2022), which also provide details on observing times and conditions as well as a more detailed description of the data reduction process[2].
Note that all the velocities mentioned in the text or in the figures are provided in the heliocentric frame.

[1] https://tbl.omp.eu/

[2] Beyond a 2-year proprietary embargo, and up to technical issues, all these data is available through PolarBase (http://polarbase.irap.omp.eu/).

3. Period search

Attempting to identify periods in an astrophysical context faces the challenge of unevenly spaced observed data. To overcome this hurdle, we used the Lomb-Scargle periodogram (Lomb 1976; Scargle 1982). This method involves fitting sinusoids to the data using least-squares with frequency sampled between the first and last observation. The quality of the fit determines the power attributed to a frequency. We applied this technique to the LSD profiles of Stokes I, U, Q and to the total linear polarization of Betelgeuse observed by the TBL over a span of 10 years (2014-2024). However, the dataset available post-dimming is insufficient to produce meaningful periodograms. Therefore, our focus was on periodograns computed exclusively from data obtained before the great dimming, covering the period from 2014 to the end of 2019.

3.1. Variability of the Stokes parameters

We first computed the Lomb-Scargle periodogram at each wavelength of the LSD profile, ranging from -25 km/s to +60 km/s to cover the entire signal present in the LSD profile. López Ariste et al. (2018) identified the most blueshifted signal towards -20 km/s and interpreted it as the maximum velocity of the rising plasma. The most redshifted signal was often found at +40 km/s, interpreted as the rest velocity of the star. Sometimes, signals at velocities greater than +40 km/s can be found, which can be interpreted either as dark and cold plasma falling back to Betelgeuse or as rising plumes of plasma located on the hidden face of Betelgeuse, ascending so high that they appear above the limb (López Ariste et al. 2023, for the case of the RSG μCep).

Figures 1,2,3 and 4 show the Lomb-Scargle periodogram of the LSD profile for Stokes I, Stokes Q, Stokes U and the total linear polarization, respectively. In each figure, the upper panel depicts the Lomb-Scargle periodogram of each velocity bin (black line) along with the total average (red line). The green line represents the window function. The lower panel shows the Lomb-Scargle periodogram for each velocity bin, with the white dotted lines marking the 400 and 200 d periods for reference. The right panel represents the mean profile of each Stokes parameter at each velocity bin.

Intensity.pdf

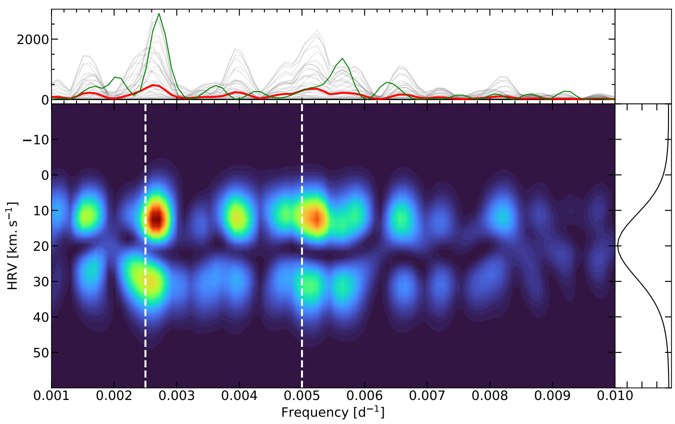

Fig. 1. Lomb-Scargle periodogram of the LSD profile of intensity. The upper panel is the Lomb-Scargle periodogram for each velocity bin (black line) and the average (red line). The green line is the window function. In the lower panel, the two white dashed lines mark respectively the 400 d and the 200 d periods. The right panel is the average intensity profile for each velocity bin.

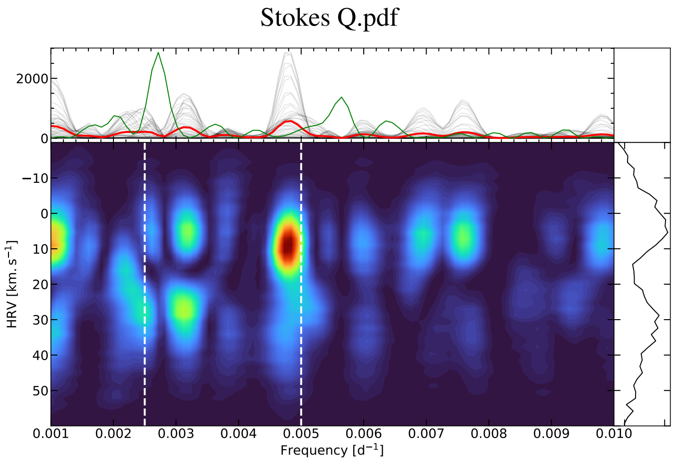

Fig. 2. Same as Fig. 1 for Stokes Q.

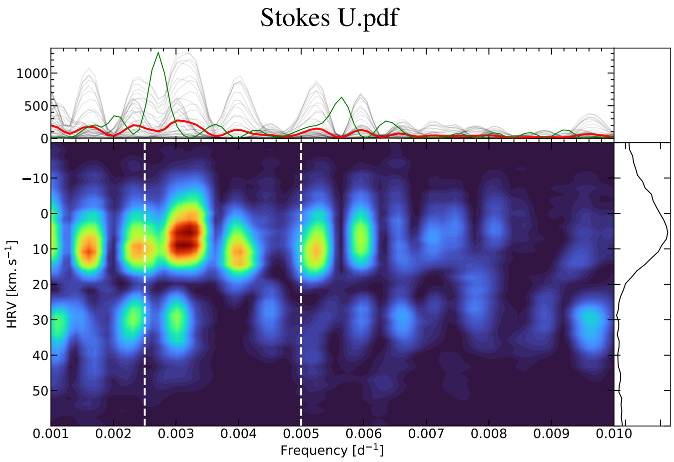

Fig. 3. Same as Fig. 1 for Stokes U.

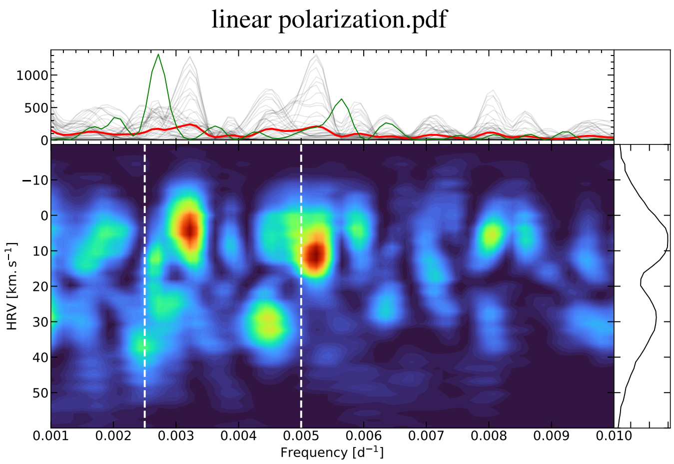

Fig. 4. Same as Fig. 1 for the total linear polarization: $\sqrt{Q^2 + U^2}$.

Examining Fig.1, which shows the Lomb-Scargle periodogram of the LSD of the intensity profile, we observe that the 400 and 200 d periods seem to be captured by the periodogram. However, the 400 d period is uncomfortably close to the peak of the window function. Furthermore, both periods are located at the same HRV and in the blue wing of the profile. Interestingly, Mathias et al. (2018) previously found this 200 d periodicity in spectroscopic observation, despite of a shorter observation period.

Figures 2 and 3 display the Lomb-Scargle periodograms of Stokes Q and U. These periodograms exhibit significant differences compared to the intensity one. In Fig. 2, a prominent signal is evident around 200 d. Regarding Stokes U in Fig. 3, it appears that the primary period is approximately 0.003 d^{-1} (equivalent to 330 d). Although other periods, such as those at 200 d or 250 d (0.004 d^{-1}) are present, but are difficult to trust. From both periodograms of Stokes Q and U, we recover the 200 d period, and also the 330 d period is notable, which aligns closely with the 400 d period reported in the literature and is in agreement with the timescale of the hysteresis loop reported by Kravchenko et al. (2019). Figure 4 shows the Lomb-Scargle periodogram of $\sqrt{Q^2 + U^2}$, representing the total linear polarization of Betelgeuse. This periodogram confirms the significant powers at both 330 d and 200 d, consistent with the periodograms of Stokes Q and U.

3.2. Variability of the polarimetric imaging

Using linear polarization, López Ariste et al. (2018) successfully reconstructed images of Betelgeuse, which have been compared favourably to inteferometric images obtained by Montargès et al. (2016). The images are produced by finding the brightness distribution that better fits the observed linear polarization LSD profile using a Marquardt-Levenberg minimisation.

Betelgeuse is observed, on average, every month by the TBL, enabling the tracking of its surface activity through this technique of polarimetric imaging. This technique has previously allowed for the estimation of the size and the lifetime of convective cells on the surface (López Ariste et al. 2018). From these images, we computed a photo-center, a quantity sensitive to the size and number of convective cells. A homogeneous star will have a photo-center displacement coinciding with the barycenter of the star, whereas a star with one or two large convective cells will exhibit a more siginificant photo-center displacement, up to a few percent of the stellar radius in the case of RSGs (Chiavassa et al. 2022).

Since the photo-center is linked to surface convection, it is worth checking for periods in its dynamics over the 5 years of observations of Betelgeuse before the dimming. While these periods may overlap with those presented in the previous section, they are likely to capture additional aspects of the phenomena at work.

However, before proceeding to search for periods in the displacement of the photo-center, it is important to address a key issue regarding the interpretation of such images. Linear polarization suffers from a 180° degree ambiguity, as mentioned in Aurière et al. (2016). Consequently, our images can be rotated by 180° degree, and the brightness distribution will still fit the observed LSD polarization profiles. If each observation were treated independently, the algorithm's solution could be any of the possible ambiguous solutions. To ensure continuity between the image series, for a given day, we use the brightness distribution of the previous day as the initial point of the fitting iteration. The first image in the series begins its minimisation iteration with a random brightness distribution. Although we can produce a series of consistent images, it is important to keep in mind that the photo-center displacement computed from the series will be affected by the initial image. To overcome this issue, we computed the photo-center displacement from 100 different time series, each starting from a different initial image. This approach aims to recover ensemble properties independent of the choice of the first image.

Photo-center.pdf

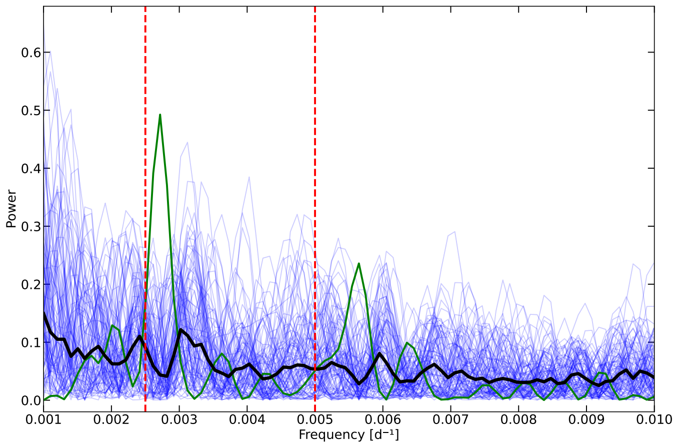

Fig. 5. Lomb-Scargle periodogram of the 100 photo-center displacement of Betelgeuse. Each blue lines correspond to a Lomb-Scargle periodogram of one photo-center displacement. The black line is the average of the 100 periodogram. The red dashed lines represent the 400 and 200 d period respectively (from left to right). The green line is the window function.

Figure 5 shows the Lomb-Scargle periodogram of the photo-center displacement for each of the 100 series (blue lines) and the average Lomb-Scargle periodogram (black line). The red dashed lines indicate the 400 and 200 d periods, respectively. Similar to previous figures, the window function is represented by the green line. Interestingly, we find two peaks around the 400 d period in the periodogram, although they are not individually significant to confirm the presence of such period. However, these peaks are consistent with the findings of the previous section. Since polarimetry imaging involves only surface convection, this provides further support for a variability being explained by surface convection alone.

3.3. Variability of the light curve

After examining the periods identified by the Lomb-Scargle technique in the polarization data obtained by the TBL over the last years before the dimming, it is worth contextualizing them alongside the periods traditionally identified in light curves over the same period of time. Two aspects are of our interest in this comparison: the behaviour of the light curve before and after the great dimming.

We have retrieved the light curve of Betelgeuse in the visible from the AAVSO database for the past 10 years, as shown in Fig. 6. Before the great dimming, Betelgeuse's magnitude exhibited variations on a yearly timescale, whereas after the dimming, its variability has shortened. Figure. 6 clearly illustrates that the variability of Betelgeuse now occurs on a timescale shorter than one year. This qualitative change has been pointed out before, before the great dimming, the primary period of Betelgeuse was approximately 400 d (Kiss et al. 2006), often associated with the fundamental pressure mode. However, after the dimming, this period seems to have vanished, and only timescales shorter than 230 d are visible since (Dupree et al. 2022). No explanations have been put forth regarding this change of variability after, or perhaps because of the dimming. Consequently, we can afford

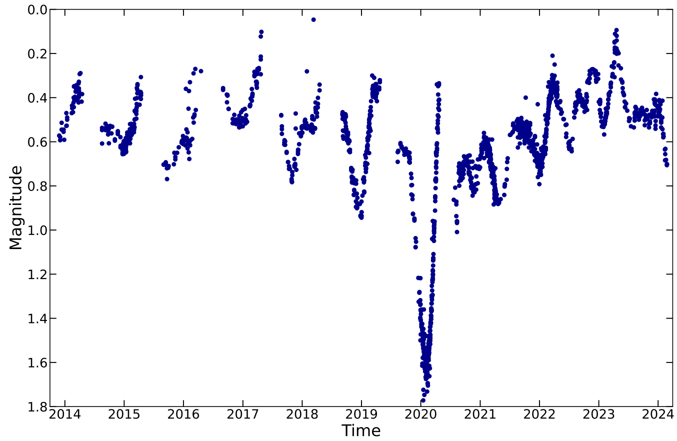

Fig. 6. Light curve of Betelgeuse from AAVSO in the V-band.

proposing alternative scenarios for the observed periodicities in the light curve (see Section 4).

We utilized the AAVSO database to search for periodicities in the light curve of Betelgeuse using the Lomb-Scargle periodogram, aiming to identify periods previously reported in the litterature. In Fig.7, we computed the periodogram from the light curve of Betelgeuse spanning from 1990 to 2024 (blue line), alongside the periodogram computed using AAVSO observations corresponding to the observation dates of the TBL (orange line) within a range of 5 days. For the periodogram since 1990, we binned the observations with an interval of 10 days, as Betelgeuse has been more observed in the 21st century (Kiss et al. 2006). Our analysis reveals the recovery of the 400 d period and also a period close to 200 d, while the other peaks are due to the windowing effect. Thus, the Lomb-Scargle periodogram succssfully identifies periods mentioned in the literature. However, when focusing on the periodogram derived from the light curve corresponding to the TBL observation dates, we fail to retrieve the periods mentioned in the literature. Hence, the small peaks present in Fig. 5 are attributed to the limited number of TBL observations.

AAVSO.pdf

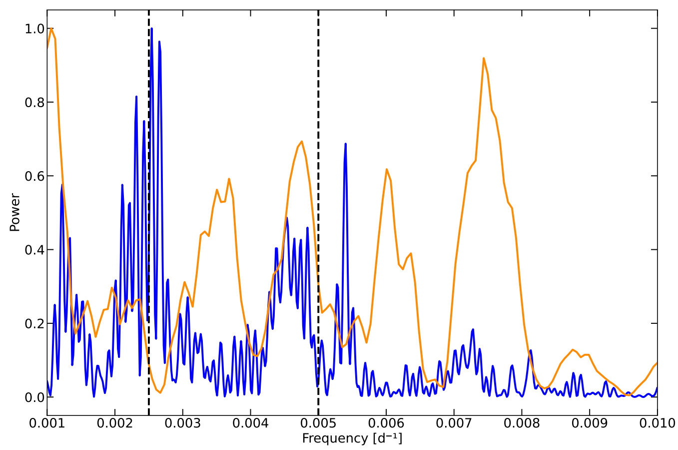

Fig. 7. Lomb-Scargle periodogram of the light curve of Betelgeuse since 1990 (blue line) and from the light curve where the dates correspond to the observation of the TBL. The two black dashed lines are respectively the 400 and 200 d periods.

4. Discussion

The presence of the same periods and, considering the time span and sparsity of the TBL data series, the larger amplitude of the peaks found in polarization data compared to those in the light curve point to a common origin, one that is rather based upon convective dynamics. Since we associate Stokes Q and U to proxies of convection, we associate the 200 d period to the typical timescales on which the Stokes parameters evolve. The LSD profiles of Stokes Q or U undergo slight changes when observing Betelgeuse monthly, but are completely overhauled on time scales of several months. The Lomb-Scargle periodograms seem to capture this spectral dynamic at periods of aproximately 200 d. Such changes in the profiles are directly linked to the dynamics of the surface, to the evolution, and movements of convective cells across the visible hemisphere. Therefore, the 200 d period appears to be related to the evolution of the convective patterns on the surface of Betelgeuse. The stronger presence of this peak in Stokes Q compared to U could be interpreted as a temporal situation of how convective patterns have been distributed in the last years.

The other period found in the total linear polarization and Stokes U, the 330 d periods, is not so far from the 400 days period often mentioned in the literature (e.g Kiss et al. (2006) found a period of 388 ± 30 d). It has been shown by López Ariste et al. (2018) that large convective cells can persist for one to two years. Thus, the 330 d period could be associated to the timescale on which the largest granules evolve. This characteristic timescale has also been observed in the numerical simulations and might play an important role in determining stellar distances through the displacement of the photo-center (Chiavassa et al. 2022). Once again, we observe the 330 d periodicity to be more prominent in Stokes U than in Q, what may unravel a random situation due to convective motions in the last years. This interpretation aligns with the work of Gray (2008), who attributed the 400 d period to large convective cells.

Regarding the Stokes I profile, it seems to correspond to the 400 d period, but is uncomfortably close to a peak of the window function of the TBL, making this peak difficult to trust. A secondary peak close to 200 d is also present in the Stokes I profile. Since we are able to recover the 200 d period in the Stokes parameters, we attribute this period to convective timescales. Up to this point, the model developed to interpret linear polarization involves only surface convection, which is why we interpret the 200 d period as the convective timescale of the smallest structures, while the 400 d period corresponds to the timescale of the largest structures.

Before summing up the results of our work, we can afford to explain the variability of Betelgeuse after the great dimming with surface convection. RSGs experience mass loss event, where plasma is ejected into the interstellar medium (Josselin & Plez 2007). These events have been inferred in RSG such as μCep, where López Ariste et al. (2023) found an excess of linear polarization beyond the limb of the star, attributing it to rising plumes of plasma in the back hemisphere of the star. In the case of Betelgeuse, the excess of linear polarization beyond the limb is rare and not as pronounced as those observed in μCep. Also, they do not change the variability of the star. However, since the great dimming, the variability of Betelgeuse has changed. This suggests that the great dimming differed significantly from the usual mass loss event, that it hustled the dynamics of the photosphere.

In a scenario where the variability of Betelgeuse is primarily governed by convection, before the great dimming, the variability of the star was associated to the typical timescale at which convection occurs: approximately 200 d for the small structures and roughly 350 d for the large structures. The great dimming affected the behaviour of the photosphere in such a way that the largest structures no longer evolved on a timescale around 350 d, but rather on the timescale of the smallest convective structures, around 200 d. We hypothesise that since the great dimming event, the photosphere has not returned to equilibrium, and the largest convective structures have been disrupted by the turbulent motion of the photosphere. Consequently, identifying periods after the great dimming is hard, which Dupree et al. (2022) noticed. We expect that the 400 d variability will gradually reappear in the coming years as the photosphere returns to equilibrium. However, it is essential to note that this scenario is speculative but provides a rough explanation of how convective activity could lead to a change in variability since the great dimming. A more detailed explanation of this variability change falls beyond the scope of this paper and is left for future research.

5. Conclusion

The main result presented in this work is that the same periods identified in the light curve of Betelgeuse are also observed in the intensity and polarization spectra measured with the TBL. Traditionally, periods in the light curve have been associated to pulsations due to pressure modes. However, the interpretation of the linear polarization profiles is made in terms of convective structures in the atmosphere of Betelgeuse. We propose that the true reason for the observed periodicities in both the light curve and spectropolarimetric observations lies within these convective structures and their temporal evolution. This is the main conclusion of our work: since we are able to recover the different periods in the linear polarization profiles, we associate the 200 d periodicity to convective dynamics, while the 400 d periodicity is linked to convective timescales of the largest granules. This conclusion concurs with the scenario proposed by Gray (2008), attributing the variability of Betelgeuse to surface convection.

Although of secondary importance, we can speculate on the phenomena underlying the change in variability before and after the great dimming event. We hypothesize that the great dimming event disrupted the dynamics of the photosphere, leading to the destruction of the largest granules by the turbulent motions caused by the non-equilibrium of the photosphere. Since this event, the variability of Betelgeuse has quickened in adequacy with the timescale of smaller convective cells, around 200 d. If this scenario is correct, we shall expect in the coming future, the re-emergence of the 400 d variability as the dominant period once the photosphere returns to some form of equilibrium. Longer time series of spectropolarimetric observations of Betelgeuse will be necessary to provide further insights into this phenomenon.

Acknowledgements. This work was supported by the "Programme National de Physique Stellaire" (PNPS) of CNRS/INSU co-funded by CEA and CNES. We acknowledge support from the French National Research Agency (ANR) funded project PEPPER (ANR-20-CE31-0002). We acknowledge the observers of the AAVSO International Database who provided more data than enough to produce this work.

References

Aurière, M., López Ariste, A., Mathias, P., et al. 2016, Astronomy and Astrophysics, 591, A119

Chiavassa, A., Kudritzki, R., Davies, B., Freytag, B., & De Mink, S. E. 2022, Astronomy & Astrophysics, 661, L1
Donati, J.-F., Semel, M., Carter, B. D., Rees, D. E., & Collier Cameron, A. 1997, Monthly Notices of the Royal Astronomical Society, 291, 658
Dupree, A. K., Strassmeier, K. G., Calderwood, T., et al. 2022, The Astrophysical Journal, 936, 18
Gray, D. F. 2008, The Astronomical Journal, 135, 1450, aDS Bibcode: 2008AJ....135.1450G
Guinan, E., Wasatonic, R., Calderwood, T., & Carona, D. 2020, The Astronomer's Telegram, 13512, 1, aDS Bibcode: 2020ATel13512....1G
Harper, G. M., Guinan, E. F., Wasatonic, R., & Ryde, N. 2020, The Astrophysical Journal, 905, 34
Jadlovský, D., Krtička, J., Paunzen, E., & Štefl, V. 2023, New Astronomy, 99, 101962
Josselin, E. & Plez, B. 2007, Astronomy and Astrophysics, 469, 671
Joyce, M., Leung, S.-C., Molnár, L., et al. 2020, The Astrophysical Journal, 902, 63
Kiss, L. L., Szabo, G. M., & Bedding, T. R. 2006, Monthly Notices of the Royal Astronomical Society, 372, 1721
Kravchenko, K., Chiavassa, A., Van Eck, S., et al. 2019, Astronomy & Astrophysics, 632, A28
Kravchenko, K., Jorissen, A., Van Eck, S., et al. 2021, Astronomy & Astrophysics, 650, L17
Lomb, N. R. 1976, Astrophysics and Space Science, 39, 447, aDS Bibcode: 1976Ap&SS..39..447L
López Ariste, A., Georgiev, S., Mathias, P., et al. 2022, Three-dimensional imaging of convective cells in the photosphere of Betelgeuse, Tech. rep., publication Title: arXiv e-prints ADS Bibcode: 2022arXiv220212011L Type: article
López Ariste, A., Mathias, P., Tessore, B., et al. 2018, Astronomy and Astrophysics, 620, A199
López Ariste, A., Wavasseur, M., Mathias, P., et al. 2023, Astronomy and Astrophysics, 670, A62, aDS Bibcode: 2023A&A...670A..62L
Mathias, P., Aurière, M., López Ariste, A., et al. 2018, ArXiv e-prints, arXiv:1804.01831
Montargès, M., Cannon, E., Lagadec, E., et al. 2021, Nature, 594, 365, number: 7863 Publisher: Nature Publishing Group
Montargès, M., Kervella, P., Perrin, G., et al. 2016, Astronomy & Astrophysics, 588, A130
Scargle, J. D. 1982, The Astrophysical Journal, 263, 835
Schwarzschild, M. 1975, The Astrophysical Journal, 195, 137
Stothers, R. 1969, The Astrophysical Journal, 156, 541
Stothers, R. B. 2010, The Astrophysical Journal, 725, 1170
Wood, P. R., Olivier, E. A., & Kawaler, S. D. 2004, The Astrophysical Journal, 604, 800